Journal of Magnetics 23(2), 179-191 (2018)

ISSN (Print) 1226-1750
ISSN (Online) 2233-6656
https://doi.org/10.4283/JMAG.2018.23.2.179

Hemodynamic Flow in a Vertical Cylinder with Heat Transfer: Two-phase Caputo Fabrizio Fractional Model

Farhad Ali[1,2]*, Anees Imtiaz[3], Ilyas Khan[4], and Nadeem Ahmad Sheikh[3]

[1]*Computational Analysis Research Group, Ton Duc Thang University, Ho Chi Minh City, Vietnam*
[2]*Faculty of Mathematics and Statistics, Ton Duc Thang University, Ho Chi Minh City, Vietnam*
[3]*Department of Mathematics, City University of Science and Information Technology, Peshawar, Khyber Pakhtunkhwa, Pakistan*
[4]*Basic Engineering Sciences Department, College of Engineering Majmaah University, Majmaah 11952, Saudi Arabia*

(Received 29 January 2018, Received in final form 29 May 2018, Accepted 29 May 2018)

In blood, the concentration of red blood cells varies with the arterial diameter. In the case of narrow arteries, red blood cells concentrate around the centre of the artery and there exists a cell-free plasma layer near the arterial wall due to Fahraeus-Lindqvist effect. Due to non-uniformity of the fluid in the narrow arteries, it is preferable to consider the two-phase model of the blood flow. The present article analyzes the heat transfer effects on the two-phase model of the unsteady blood flow when it flows through the stenosed artery under an external pressure gradient. The direction of the artery is assumed to be vertical and the magnetic field is applied along the radial direction of the artery. Blood is considered as a non-Newtonian Casson fluid with uniformly distributed magnetic particles. Both the blood and magnetic particles are moving with distinct velocities. This two-phase problem is modelled using the Caputo-Fabrizio derivative approach and then solved for an exact solution using joint Laplace & Hankel transforms. Effects of pertinent parameters such as Grashoff number, Prandtl number, Casson fluid parameter and fractional parameters, and magnetic field on blood velocity and particle velocity have been shown graphically for both large and small values of time. Both velocity profiles increase with the increase of Grashoff number and Casson fluid parameter and reduce with the increase of magnetic field and Prandtl number. The behaviour of temperature is studied for different values of the fractional parameter.

Keywords : two-phase blood flow, magnetic particles, heat transfer, fractional derivative, Joint Laplace and Hankel transforms

1. Introduction

Biomagnetic fluid dynamic (BFD) is an interesting area of research and have extraordinary applications in bioengineering and medical sciences. The kinematics and dynamics of the body fluid in human, animals and plants are described by BFD. In humans, hemodynamics deals with the body fluids. Modern BFD measures and analyzes local time-dependent velocities and flow in blood vessels [1-3]. The interest in this field includes the development of using magnetic particles as drug carriers and cancer tumour treatment using magnetic hyperthermia, reduction of bleeding during surgeries, construction of magnetic tracers and magnetic devices for cell separation [4-8]. Mostly, BFD problems are nonlinear, therefore, a limited number of analytical solutions are available and most such problems are studied numerically [9-15].

To examine the biomagnetic fluid flow under the external applied magnetic field, the formulation of mathematical model plays a crucial role. The BFD model was proposed by Haik *et al.* [16] for the investigation of biomagnetic fluid flow. This model is similar to one of the Ferro hydrodynamics (FHD), and the biological fluids are considered as electrically non-conducting magnetic fluid (Ferrofluids), however, blood exhibits high electrical conductivity [17].

The BFD comprises for the discussion of non-Newtonian fluids, like blood. Blood is the most suitable biomagnetic fluid and it behaves like a magnetic fluid [18, 19]. The magnetic behaviour of the blood is due to the complex intercellular protein interaction, cell membrane and haemoglobin, and they are formed of iron oxides,

*Corresponding author: Tel: +92-301-8882933
Fax: +92-91-2609500, e-mail: farhad.ali@tdt.edu.vn

while the magnetic property of the blood is affected from the oxygenation state [20]. Blood behaves as diamagnetic material when it is oxygenated; however, when it is deoxygenated, it behaves like paramagnetic material [21]. Blood can be viewed as a suspension of magnetic particles in non-magnetic plasma [22, 23]. As blood is a suspension of red blood cells in plasma, it carries on a non-Newtonian behaviour, but many researchers have studied the blood flow in arteries either Newtonian or non-Newtonian [24, 25]. At the point when blood moves through larger arteries at higher shear stress, it shows Newtonian behaviour but in smaller arteries at lower shear stress, it shows non-Newtonian behaviour [26]. But blood may behave as a non-Newtonian fluid in particular situation as discussed in [27-29].

The non-Newtonian example of blood is Casson fluid [30]. More exactly, Casson fluid is a shear thinning liquid which is assumed to have an infinite viscosity at zero rates of shear, the yield stress at which flow is impossible [31]. For a mathematical model of blood flow through narrow arteries at lower share stress, Casson fluid model has been discussed by many researchers [32]. Charm and Kurland [33] investigated in their experimental discoveries that the Casson fluid model could be the best illustrative of blood when it flows through narrow arteries at lower shear rates and that it could be connected to human blood at an extensive variety of Hematocrit and shear rates. Merrill *et al.* [34] found that the Casson fluid model verifies sufficient flow behaviour of blood in cylindrical tubes with the diameter of 130-1000 μm.

Blood is treated as an MHD fluid which helps to control the blood pressure and has likely corrective use in the infection of heart and vein. Measurements have also been performed for the estimation of the magnetic susceptibility of blood which was found to be 3.5×10^{-6} and -6.6×10^{-7} for the venous and arterial blood, respectively [35]. Experiments have been performed using a relatively weak magnetic field 1.8 Tesla and low temperatures (75-295) K [36]. Strong magnetic fields 8 Tesla were also used on a living rat and the consequence was the reduction of the blood flow and the temperature of the rat [37]. Also, experiments have shown that for a magnetic field of the same strength 8 Tesla, the flow rate of human blood in a tube was reduced by 30% [38]. Use of electromagnetic field in biomathematical research was first given by Kolin [39]. Afterwards, Barnothy and Sumegi [40] revealed that the organic frameworks are influenced by the utilization of an external magnetic field. Haldar *et al.* [41] concentrated on the impact of externally applied homogeneous magnetic field on the stream qualities of blood through a single constricted blood vessel in the presence of erythrocytes.

An extensive amount of work on the two-phase flow of fluids and their mathematical models have been discussed by many researchers to investigate the interaction and behaviour of the flow. Cokelet & Goldsmith [42] discussed the two-phase flow of blood through small tubes at low shear stress compared the experimental results with the predicted steady two-phase flow model. Recebli and Kurt [43] investigated unsteady flow along a horizontal glass pipe in the presence of the magnetic and electrical fields and got analytical solutions by Laplace and D'Alembert method. Gedik *et al.* [44] studied numerically the unsteady viscous incompressible and electrical conduction of two-phase fluid flow in circular pipes with external magnetic and electrical fields. The magnetic field decreases the velocity of both fluid phases, whereas the electrical field alone has no any impact on two-phase flow. Sharan *et al.* [45] numerically discussed the two-phase model for flow of blood in narrow tubes with increased effective viscosity near the wall.

Recently, many researchers have used the fractional derivatives for the solution of different problems, while in past the classical derivatives were used in mathematical formulations of problems and the idea of fractional derivatives was ignored due to its complexities [46-48]. Abro *et al.* [49] used the concept of fractional derivative to convection flow of MHD Maxwell fluid in a porous medium over a vertical plate. Abro *et al.* [50] discussed the dual thermal analysis of the magnetohydrodynamic flow of nanofluids via fractional derivative approach. Shah *et al.* [51] extended the work of [52] by applying the Caputo's time fractional derivative to study the magnetic particles on blood flow. Ali *et al.* [53] extended the work of [51] by utilizing Caputo's time fractional derivative to discuss the Casson fluid model for blood flow in a horizontal cylinder. Recently, Ali *et al.* [54] extended the work of [53] by using new fractional derivative known as Caputo-Fabrizio time fractional derivative to discuss the flow of magnetic particles in blood with Isothermal heating.

Based on the above discussion, this article aims to study the effect of the external applied magnetic field on two-phase blood flow of fractional Casson fluid in a vertical stenosed artery with isothermal heating. The mixed convection has produced by the external pressure gradient and buoyancy forces. The joint Hankel and Laplace transformation have been used for the exact solutions of the blood velocity, magnetic particle velocity and for the temperature, as the fluid flow is through the cylindrical tube. The effects of different fluid parameters have been discussed graphically for both the velocities and temperature.

Nusselt number has been calculated and shown in tabular form.

2. Statement of the Problem

The magnetic blood flow is considered in a vertical stenosed artery of radius R_0 taken along the *z-axis*. The magnetic particles are uniformly distributed throughout the fluid. The blood flow is along the *z-axis* and is due to the oscillating pressure gradient and buoyancy forces caused by the convective heat transfer. The applied magnetic field is taken in a transverse direction to the blood flow as shown in Fig. 1. The blood flow is originated due to the sudden jerk of the artery and the magnetic particles are also moving with a specific velocity $U_0\left(1-e^{-\frac{K}{m}t}\right)$. Due to the small Reynolds number the induced magnetic field has been neglected [55]. At the time $t = 0$, the fluid (blood), particles and cylinder are at rest and the temperature is ambient T_∞. At the time $t = 0^+$, the fluid and particle start motion with velocity U_0 and the temperature rises from ambient to wall temperature T_w.

The flow model can be well described with Navier-Stokes equations, Newton's second law of motion and Maxwell's relations which explain the fluid flow and particles motion. The Maxwell equations of the electro-magnetic field can be defined as

$$\nabla.\vec{B}=0,\ \nabla\times\vec{B}=\mu_0\vec{J},\ \nabla\times\vec{E}=-\frac{\partial\vec{B}}{\partial t}, \tag{1}$$

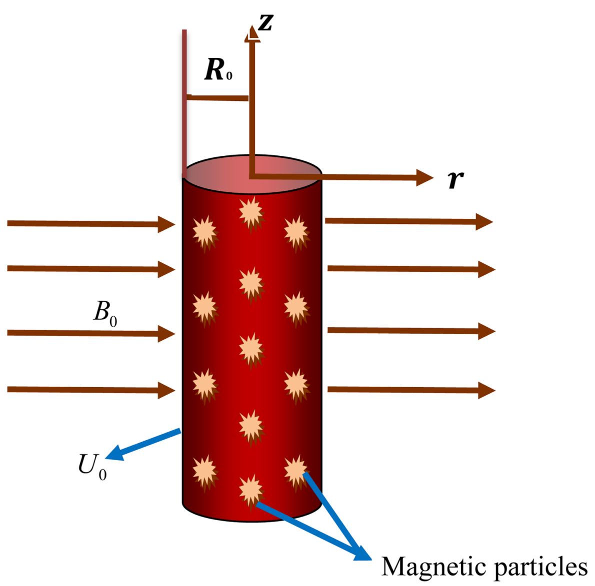

Fig. 1. (Color online) Schematic diagram.

where μ_0 is the magnetic permeability, $\vec{J}$ is the current density, $\vec{E}$ is the electric field and $\vec{B}$ is the magnetic field. The density of the electric current can be given by Ohm's law

$$\vec{J}=\sigma(\vec{E}+\vec{V}\times\vec{B}), \tag{2}$$

σ is the electrical conductivity, $\vec{E}$ is the electric field intensity, $\vec{B}$ is the magnetic flux density, $\vec{V}$ is the velocity vector. The electromotive force F_{emag} can be expressed as

$$\vec{F}_{emag}=\vec{J}\times\vec{B}=\sigma(\vec{E}+\vec{V}\times\vec{B})\times\vec{B}=-\sigma B_0^{\,2}\,w(r,t)\vec{k}, \tag{3}$$

where $\vec{k}$ is the unit vector along z-direction and $\vec{V}=w(r,t)\vec{k}$ is the velocity of blood along the axis of the circular cylinder.

The unsteady Casson fluid flow of blood in an axisymmetric cylinder [53] is given by:

$$\begin{aligned}\frac{\partial w(r,t)}{\partial t}&=-\frac{1}{\rho}\frac{\partial p}{\partial z}+\nu\left(1+\frac{1}{\beta}\right)\left(\frac{\partial^2 w(r,t)}{\partial r^2}+\frac{1}{r}\frac{\partial w(r,t)}{\partial r}\right)\\&+\frac{KN}{\rho}\left(w_1(r,t)-w(r,t)\right)\\&-\frac{\sigma B_0^2}{\rho}w(r,t)\pm g\beta_T(T-T_\infty),\end{aligned} \tag{4}$$

the oscillating pressure gradient is given by [53]

$$-\frac{\partial p}{\partial z}=Q_0+Q_1\cos\omega t, \tag{5}$$

where $w(r, t)$ is the blood velocity, $w_1(r, t)$ is the particle velocity, ρ is the density of the fluid, ν is the kinematic viscosity, $\beta=\frac{\mu_B\sqrt{2\pi_c}}{\tau_r}$ is the Casson fluid parameter, μ_B is the plastic dynamic viscosity, τ_r is the yield stress of fluid, π_c is the critical value of this product based for the non-Newtonian model, K is the Stokes constant, N is the number of magnetic particles per unit volume, σ is the electrical conductivity, B_0 is the applied magnetic field.

The term $\frac{KN}{\rho}\left(w_1(r,t)-w(r,t)\right)$ is the force between the fluid and particle due to relative motion, g is the gravitational acceleration, β_T is the coefficient of thermal expansion, T is the temperature of the fluid, T_∞ is the ambient temperature, Q_0, Q_1 are the amplitudes of the systolic and diastolic pressure gradient, The flow of magnetic particle is conducted by Newton's second law of motion [53]:

$$m\frac{\partial w_1}{\partial t} = K\left(w(r,t) - w_1(r,t)\right), \tag{6}$$

where m represents the mass of the magnetic particles.

The energy equation is given by [54]:

$$\frac{1}{\alpha_1}\frac{\partial T(r,t)}{\partial t} = \frac{\partial^2 T(r,t)}{\partial r^2} + \frac{1}{r}\frac{\partial T(r,t)}{\partial r}; \quad t>0, r\in(0,R_0), \tag{7}$$

where $\alpha_1 = \dfrac{k}{\rho C_p}$.

with respect to the following physical initial and boundary conditions:

$$\left.\begin{aligned} & w(r,0)=0 \quad , \quad w_1(r,0)=0 \\ & w(R_0,t)=U_0 \quad , \quad w_1(R_0,t)=U_0\left(1-e^{-\frac{K}{m}t}\right) \\ & T(r,0)=T_\infty \quad , \quad T(R_0,t)=T_w \\ & \left.\frac{\partial w}{\partial r}\right|_{r=0}=0 \end{aligned}\right\}, \tag{8}$$

where K is the Stokes constant.

By using the dimensionless variables

$$\begin{aligned} & r^* = \frac{r}{R_0},\ t^* = \frac{\nu t}{R_0^2},\ w^* = \frac{w}{U_0},\ w_1^* = \frac{w_1}{U_0}, \\ & \theta = \frac{T-T_\infty}{T_w - T_\infty},\ Q_0^* = \frac{Q_0 R_0^2}{\mu U_0},\ Q_1^* = \frac{Q_1 R_0^2}{\mu U_0}, \end{aligned} \tag{9}$$

into equations (4-8) after dropping the * sign, we obtain:

$$\begin{aligned} \frac{\partial w}{\partial t} &= \left(Q_0 + Q_1\cos\omega t\right) + \left(1+\frac{1}{\beta}\right)\left(\frac{\partial^2 w(r,t)}{\partial r^2} + \frac{1}{r}\frac{\partial w(r,t)}{\partial r}\right) \\ &\quad + P_c\left(w_1(r,t) - w(r,t)\right) - M^2 w(r,t) \pm Gr\theta(r,t), \end{aligned} \tag{10}$$

$$\frac{\partial w_1(r,t)}{\partial t} = P_m\left(w(r,t) - w_1(r,t)\right), \tag{11}$$

$$\frac{\partial \theta(r,t)}{\partial t} = \frac{1}{\Pr}\left(\frac{\partial^2 \theta(r,t)}{\partial r^2} + \frac{1}{r}\frac{\partial \theta(r,t)}{\partial r}\right), \tag{12}$$

$$\left.\begin{aligned} & w(r,0)=0 \quad , \quad w_1(r,0)=0 \\ & w(1,t)=1 \quad , \quad w_1(1,t)=\left(1-e^{-\frac{t}{P_m}}\right) \\ & \theta(r,0)=0 \quad , \quad \theta(1,t)=1 \end{aligned}\right\}, \tag{13}$$

$$P_c = \frac{KNR_0^2}{\rho\nu},\ M = \frac{\sigma B_0^2 R_0^2}{\rho\nu},\ Gr = \frac{g\beta_T(T_w - T_\infty)R_0^2}{\nu U_0}, \quad \Pr = \frac{\nu}{\alpha_1},\ P_m = \frac{m\nu}{KR_0^2},$$

where P_c is the non-dimensional parameter for the particle concentration, P_m is the particles mass parameter, M is the magnetic parameter, Gr is the Grashof number and Pr is the Prandtl number.

In order to convert classical time derivative to Caputo-Fabrizio fractional time derivative the equations (10-12) reduce to:

$$\begin{aligned} D_t^\alpha w(r,t) &= \left(Q_0 + Q_1\cos\omega t\right) + \left(1+\frac{1}{\beta}\right)\left(\frac{\partial^2 w(r,t)}{\partial r^2} + \frac{1}{r}\frac{\partial w(r,t)}{\partial r}\right) \\ &\quad + P_c\left(w_1(r,t) - w(r,t)\right) - Mw(r,t) \pm Gr\theta(r,t), \end{aligned} \tag{14}$$

$$D_t^\alpha w_1(r,t) = P_m\left(w(r,t) - w_1(r,t)\right), \tag{15}$$

$$D_t^\alpha \theta(r,t) = \frac{1}{\Pr}\left(\frac{\partial^2 \theta(r,t)}{\partial r^2} + \frac{1}{r}\frac{\partial \theta(r,t)}{\partial r}\right), \tag{16}$$

where Caputo Fabrizio time fractional derivative is defined as

$$D_t^\alpha f(r,t) = \frac{N(\alpha)}{1-\alpha}\int_0^\tau \exp\left(\frac{-\alpha(\tau - t)}{1-\alpha}\right) f'(\tau)dt,\ \textit{for}\ 0<\alpha<1,$$
$$N(1) = N(0) = 1$$

3. Solution of the Problem

The Joint Laplace and Hankel transform have been used to find the exact solutions for the fractional partial differential equations.

3.1. Calculation of temperature

By applying the Laplace transform to equation (16), we get

$$\frac{a_0 q}{q+a_1}\bar{\theta}(r,q) = \frac{1}{\Pr}\left(\frac{\partial^2 \bar{\theta}(r,q)}{\partial r^2} + \frac{1}{r}\frac{\partial \bar{\theta}(r,q)}{\partial r}\right), \tag{17}$$

where $a_0 = \dfrac{1}{1-\alpha}$; $\alpha \neq 1$ and $a_1 = a_0\alpha$.

Now applying the Hankel transform of order zero and using the transformed condition we get

$$\overline{\theta_H}(r_n,q) = \frac{J_1(r_n)}{r_n q} - \frac{1}{\alpha}\frac{\Pr a_3 r_n^2 J_1(r_n)}{r_n^3(q+a_3)(a_0\Pr + r_n^2)}, \tag{18}$$

where

$$a_{2n} = a_0\Pr + r_n^2,\ a_{3n} = \frac{a_1 r_n^2}{a_2},\ a_{3n}a_{2n} = a_1 r_n^2, \quad \frac{a_1}{a_{3n}a_{2n}} = \frac{1}{r_n^2},\ \frac{a_0}{a_1} = \frac{1}{\alpha},$$

$J_0(r_n)$ is the Bessel function of zero order of first kind & r_n, n = 0, 1, ... are the positive roots of the equation [56].

Now applying the inverse Laplace transform to equation

(18), we get:

$$\overline{\theta_H}(r_n,t)=\frac{J_1(r_n)}{r_n}-\frac{1}{\alpha}\frac{\Pr a_{3n}r_n^2J_1(r_n)}{r_n^3(a_0\Pr+r_n^2)}\exp(-a_{3n}t). \quad (19)$$

Now applying inverse Hankel transform to equation (19), we get:

$$\theta(r,t)=1-2\frac{\Pr}{\alpha}\sum_{n=1}^{\infty}\frac{J_0(rr_n)a_1}{r_nJ_1(r_n)(a_0P_r+r_n^2)}\exp(-a_{3n}t). \quad (20)$$

3.2. Calculation of the velocity

By applying the Laplace transform to equations (14) & (15), we get

$$\left(\frac{a_0q}{q+a_1}\right)\overline{w}(r,q)=\frac{Q_0}{q}+\frac{Q_1q}{q^2+\omega^2}+\beta_1\left(\frac{\partial^2\overline{w}(r,q)}{\partial r^2}+\frac{1}{r}\frac{\partial\overline{w}(r,q)}{\partial r}\right)$$
$$+P_c\left(\overline{w}(r,q)-\overline{w}_1(r,q)\right)-M\overline{w}(r,q)\pm Gr\overline{\theta}(r,q), \quad (21)$$

$$\overline{w}_1(r,q)=\overline{w}(r,q)\left(\frac{q+a_1}{a_1+q(1+P_ma_0)}\right), \quad (22)$$

where $\frac{1}{\beta_0}=\left(1+\frac{1}{\beta}\right)$ and $\beta_1=\frac{1}{\beta_0}$

Now applying the finite Hankel transform of order zero to equations (21) & (22), by a famous result [57],

$$\int_0^1\left(\frac{\partial^2\overline{u}(r,q)}{\partial r^2}+\frac{1}{r}\frac{\partial\overline{u}(r,q)}{\partial r}\right)dr=(r_nJ_1(r_n)\overline{u}_H(1,q)-r_n^2)\overline{u}_H(r_n,q).$$

we get:

$$\left(\frac{a_0q}{q+a_1}\right)\overline{w_H}(r_n,q)=\left(\frac{Q_0}{q}+\frac{Q_1q}{q^2+\omega^2}\right)\frac{J_1(r_n)}{r_n}$$
$$+\beta_1\left(-r_n^2\overline{w_H}(r_n,q)+r_nJ_1(r_n)\overline{w}(1,q)\right) \quad (23)$$
$$+P_c\left(\overline{w_H}(r_n,q)-\overline{w_{1H}}(r_n,q)\right)-M\overline{w_H}(r_n,q)\pm Gr\overline{\theta}_H(r_n,q),$$

$$\overline{w_{1H}}(r_n,q)=\overline{w_H}(r_n,q)\left(\frac{q+a_1}{a_1+q(1+P_ma_0)}\right). \quad (24)$$

Incorporating the transformed condition $\overline{w}(1,q)=\frac{1}{q}$, equation (23) becomes

$$\left(\frac{a_0q}{q+a_1}\right)\overline{w_H}(r_n,q)=\left(\frac{Q_0}{q}+\frac{Q_1q}{q^2+\omega^2}\right)\frac{J_1(r_n)}{r_n}-\beta_1r_n^2\overline{w_H}(r_n,q)$$
$$+\frac{\beta_1r_nJ_1(r_n)}{q}+P_c\left(\overline{w_H}(r_n,q)-\overline{w_{1H}}(r_n,q)\right)$$
$$-M\overline{w_H}(r_n,q)\pm Gr\overline{\theta}_H(r_n,q). \quad (25)$$

By incorporating equation (24) into equation (25), we get:

$$\left(\frac{a_0q}{q+a_1}\right)\overline{w_H}(r_n,q)=\left(\frac{Q_0}{q}+\frac{Q_1q}{q^2+\omega^2}\right)\frac{J_1(r_n)}{r_n}-\beta_1r_n^2\overline{w_H}(r_n,q)$$
$$+\frac{\beta_1r_nJ_1(r_n)}{q}+P_c\left(\overline{w_H}(r_n,q)-\overline{w_H}(r_n,q)\left(\frac{q+a_1}{a_1+q(1+P_ma_0)}\right)\right)$$
$$-M\overline{w_H}(r_n,q)\pm Gr\overline{\theta}_H(r_n,q), \quad (26)$$

equation (26) can be written in simplified form by letting $Pm_1=1+Pma_0$,

$$\left(\frac{k_{0n}q^2+k_{1n}q+k_{2n}}{(q+a_1)(P_{m1}q+a_1)}\right)\overline{w_H}(r_n,q)=\overline{F_n}(q)\pm Gr\overline{\theta}_H(r_n,q)+\frac{\beta_1r_nJ_1(r_n)}{q}, \quad (27)$$

where

$$\overline{F_n}(q)=\left(\frac{Q_0}{q}+\frac{Q_1q}{q^2+\omega^2}\right)\frac{J_1(r_n)}{r_n},$$
$$k_{0n}=b_0+\beta_1r_n^2P_{m1},\ k_{1n}=b_1+\beta_1r_n^2a_1(1+P_{m1}),$$
$$k_{2n}=b_2+a_1^2r_n^2\beta_1,\ b_0=(a_0+M)P_{m1}+a_0P_cP_m,$$
$$b_1=a_1a_0(1+P_cP_m)+a_1M(1+P_{m1}),\ b_2=Ma_1^2$$

$$\overline{w_H}(r_n,q)=\overline{F_n}(q)\left(\frac{(q+a_1)(P_{m1}q+a_1)}{k_{0n}q^2+k_{1n}q+k_{2n}}\right)$$
$$\pm Gr\overline{\theta}_H(r_n,q)\left(\frac{(q+a_1)(P_{m1}q+a_1)}{k_{0n}q^2+k_{1n}q+k_{2n}}\right) \quad (28)$$
$$+\frac{\beta_1r_nJ_1(r_n)}{q}\left(\frac{(q+a_1)(P_{m1}q+a_1)}{k_{0n}q^2+k_{1n}q+k_{2n}}\right),$$

By letting $\overline{S_{0n}}(q)=\frac{\beta_1r_nJ_1(r_n)}{q}\left(\frac{(q+a_1)(P_{m1}q+a_1)}{k_{0n}q^2+k_{1n}q+k_{2n}}\right)$,

$$\overline{S_{1n}}(q)=\left(\frac{(q+a_1)(P_{m1}q+a_1)}{k_{0n}q^2+k_{1n}q+k_{2n}}\right)$$

equation (28) becomes

$$\overline{w_H}(r_n,q)=\left\{\overline{F_n}(q)\pm Gr\overline{\theta}_H(r_n,q)\right\}\overline{S_{1n}}(q)+\overline{S_{0n}}(q). \quad (29)$$

Now incorporating, $\overline{\theta_H}(r_n,q)=\frac{J_1(r_n)}{r_n}\left(\frac{1}{q}-\frac{a_0\Pr}{q+a_3}\right)$ and through simplification, equation (29) is reduced to

$$\overline{w_H}(r_n,q)=\frac{J_1(r_n)}{r_nq}+\frac{J_1(r_n)}{r_n}\overline{G_{1n}}(q)$$
$$+\overline{F_n}(q)\overline{S_{1n}}(q)\pm Gr\frac{J_1(r_n)}{r_n}\overline{S_{2n}}(q)\overline{S_{1n}}(q). \quad (30)$$

By introducing the following expressions

$$\overline{G_{1n}}(q) = \frac{J_1(r_n)}{r_n}\left\{\frac{Q_{0n}}{q} + \left(\frac{Q_{0n}}{q_{1n}-q_{2n}}\right)\frac{1}{q-q_{1n}} + \left(\frac{Q_{2n}}{q_{1n}-q_{2n}}\right)\frac{1}{q-q_{2n}}\right\},$$

$$\overline{S_{1n}}(q) = \left\{A_{1n}\frac{1}{q-q_{1n}} - A_{2n}\frac{1}{q-q_{2n}}\right\},\ \overline{S_{2n}}(q) = \left(\frac{1}{q} - \frac{a_0 \Pr}{q+a_3}\right),$$

$$Q_{0n} = \frac{k_{0n}}{k_{2n}}\left(\beta_1 r_n^2 a_1^2 - k_{2n}\right), Q_{1n} = \beta_1 r_n^2 P_{m1}\left(q_{1n} + a_1 + \frac{a_1}{P_{m1}}\right) - \beta_1 r_n^2 a_1\left(\frac{k_{0n}}{k_{2n}}a_1 q_{1n} + \frac{k_{1n}}{k_{2n}}\right),$$

$$Q_{2n} = \beta_1 r_n^2 P_{m1}\left(q_{2n} + a_1 + \frac{a_1}{P_{m1}}\right) - \beta_1 r_n^2 a_1\left(\frac{k_{0n}}{k_{2n}}a_1 q_{2n} + \frac{k_{1n}}{k_{2n}}\right),$$

$$A_{1n} = \left(\frac{a_1(1+P_{m1})q_{1n} + a_1^2}{q_{1n}-q_{2n}}\right), A_{2n} = \left(\frac{a_1(1+P_{m1})q_{2n} + a_1^2}{q_{1n}-q_{2n}}\right),$$

$$q_{1n}, q_{2n} = \frac{-k_{1n} \pm \sqrt{k_{1n}^2 - 4k_{0n}k_{1n}}}{2k_{0n}}, q_{1n} + q_{2n} = \frac{-k_{1n}}{k_{0n}}, q_{1n}.q_{2n} = \frac{k_{2n}}{k_{0n}}$$

$$k_{0n}q^2 + k_{1n}q + q_{2n} = (q-q_{1n})(q-q_{2n}),$$

Applying inverse Laplace transform to equation (30), we get

$$w_H(r_n,t) = \frac{J_1(r_n)}{r_n} + \frac{J_1(r_n)}{r_n}G_{1n}(t) + F_n(t) * S_{1n}(t) \pm Gr\frac{J_1(r_n)}{r_n}S_{2n}(t) * S_{1n}(t). \tag{31}$$

Finally applying the inverse Hankel transform to equation (31) by using the famous result [54]

$$H_0^{-1}\left(w_{1H}(r_n,t)\right) = w_1(r,t) = 2\sum_{n=1}^{\infty} w_{1H}(r_n,t)\frac{J_0(rr_n)}{J_1(r_n)},$$

we get:

$$w(r,t) = 1 + 2\sum_{n=1}^{\infty}\left(\frac{J_0(rr_n)}{J_1(r_n)r_n}\right)G_{1n}(t) + 2\sum_{n=1}^{\infty}\left(\frac{J_0(rr_n)}{J_1^2(r_n)}\right)F_n(t) * S_{1n}(t) \pm 2\sum_{n=1}^{\infty}\left(\frac{J_0(rr_n)}{J_1(r_n)r_n}\right)Gr\, S_{2n}(t) * S_{1n}(t). \tag{32}$$

Equation (24), will be written in more systematic form by taking, $P_{m1} = 1 + P_m a_0, P_{m2} = \frac{a_1}{P_{m1}}$

$$\overline{w_{1H}}(r_n,q) = \overline{w_H}(r_n,q)\left(\frac{1}{P_{m1}}\frac{q}{q+P_{m2}} + P_{m2}\frac{1}{q+P_{m2}}\right). \tag{33}$$

Now by applying inverse Laplace transform to equation (33), using the known result of Lorenzo & Hartley function [58]

$$L^{-1}\left\{\frac{q^{-\upsilon}}{q^{\alpha}+\gamma}\right\} = \Re_{\alpha,\upsilon}(-\gamma,t) = \sum_{n=0}^{\infty}\frac{(-\gamma)^n t^{(n+1)\alpha-1-\upsilon}}{\Gamma\left((n+1)\alpha-\upsilon\right)},$$

we get

Table 1. Nusselt number variation due to time and fractional parameter α).

t	α	Nu
0.1	0.2	2.438
0.1	0.5	2.383
0.1	0.7	2.302
0.1	0.9	2.165
1	0.2	2.604
1	0.5	2.902
1	0.7	3.159
1	0.9	3.491

$$w_{1H}(r_n,t) = w_H(r_n,t) * \left(\frac{1}{P_{m1}}\Re_{1,-1}(-P_{m2},t) + P_{m2}\exp(-P_{m2}t)\right), \tag{34}$$

finally applying inverse Hankel transform of order zero to equation (34), we get

$$w_1(r,t) = w(r,t) * \left(\frac{1}{P_{m1}}\Re_{1,-1}(-P_{m2},t) + P_{m2}\exp(-P_{m2}t)\right). \tag{35}$$

3.3. Rate of Heat transfer

Nusselt number measures the rate of heat transfer from the surface of the cylinder to the fluid. The Nusselt number in dimensionless form is given by:

$$Nu = -\left(\frac{\partial\theta(r,t)}{\partial r}\right)_{r=1}. \tag{36}$$

The expression of Nusselt number can easily be obtained by incorporating equation (20) into equation (36). Hence, the numerical results (using Mathcad) are computed from equation (36) and are given in Table 1.

From the above table, it can be concluded that for short interval of time and increasing values of α the heat transfer rate decreases while for large interval of time the heat transfer rate increases.

4. Graphical Results and Discussion

The impact of different fluid parameters on temperature $\theta(r, t)$, blood velocity $w(r, t)$ and particle velocity $w_1(r, t)$ has been discussed graphically by using the computational tool Mathcad. The physical sketch of the problem is shown in Fig. 1. In Fig. 2 the effect of the fractional parameter α at temperature has been discussed for different values of time. In Fig. 2(a) time is taken $t = 0.1$ and it is clearly be observed that at center of the cylinder, for higher values of α the classical fluid temperature is higher than the fractional fluid temperature while it has a reverse effect on the fluid temperature near the walls of the cylinder, and in Fig. 2(b) time is taken $t = 1$ and from

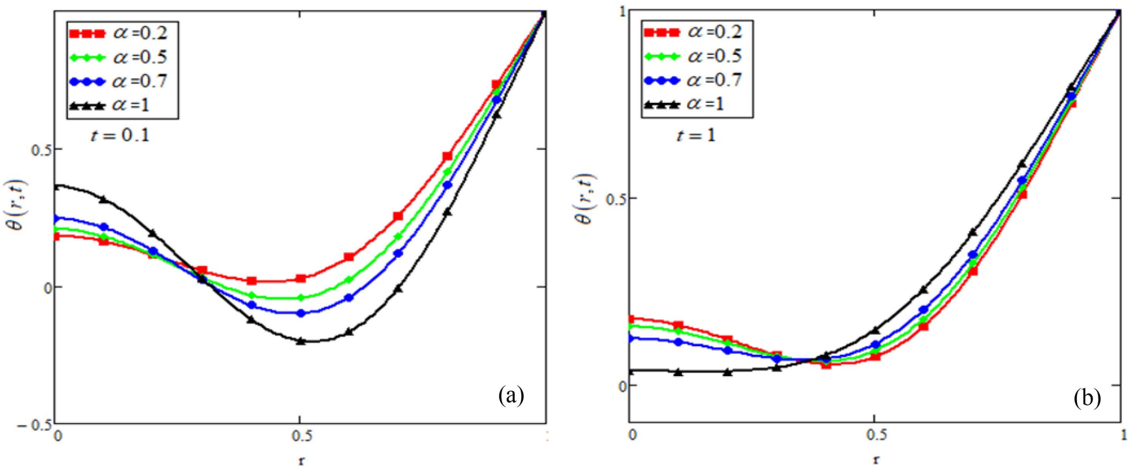

Fig. 2. (Color online) Temperature graph for different values of α when Pr=22.64.

Figure it's clearly be seen that for higher values of α the classical fluid temperature is lower than the fractional fluid temperature while it has a reverse effect on the fluid temperature near the walls of the cylinder. The graphs for blood velocity as well as for magnetic particle velocity are shown in Figs. 3-6. All these graphs are studied for the fractional parameter α. In Fig. 3 and Fig. 4, the effect of magnetic parameter M has been discussed for short and

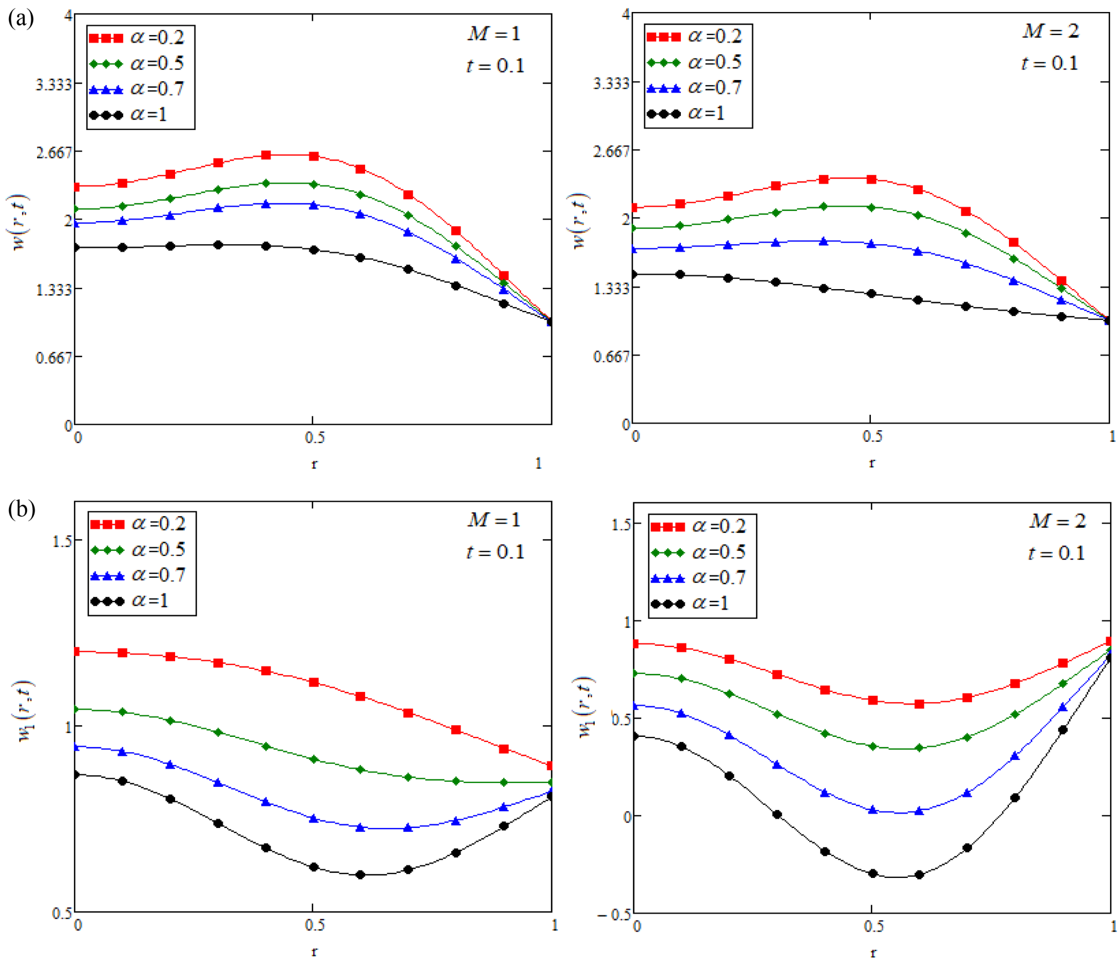

Fig. 3. (Color online) Velocity graph of Blood and Particles for different values of M for short time, when Q_0=0.3, Q_1=0.3, P_m=0.2, P_c=0.2, β= 1, $\omega = \frac{\pi}{2}$, Pr=22.64, Gr=10.

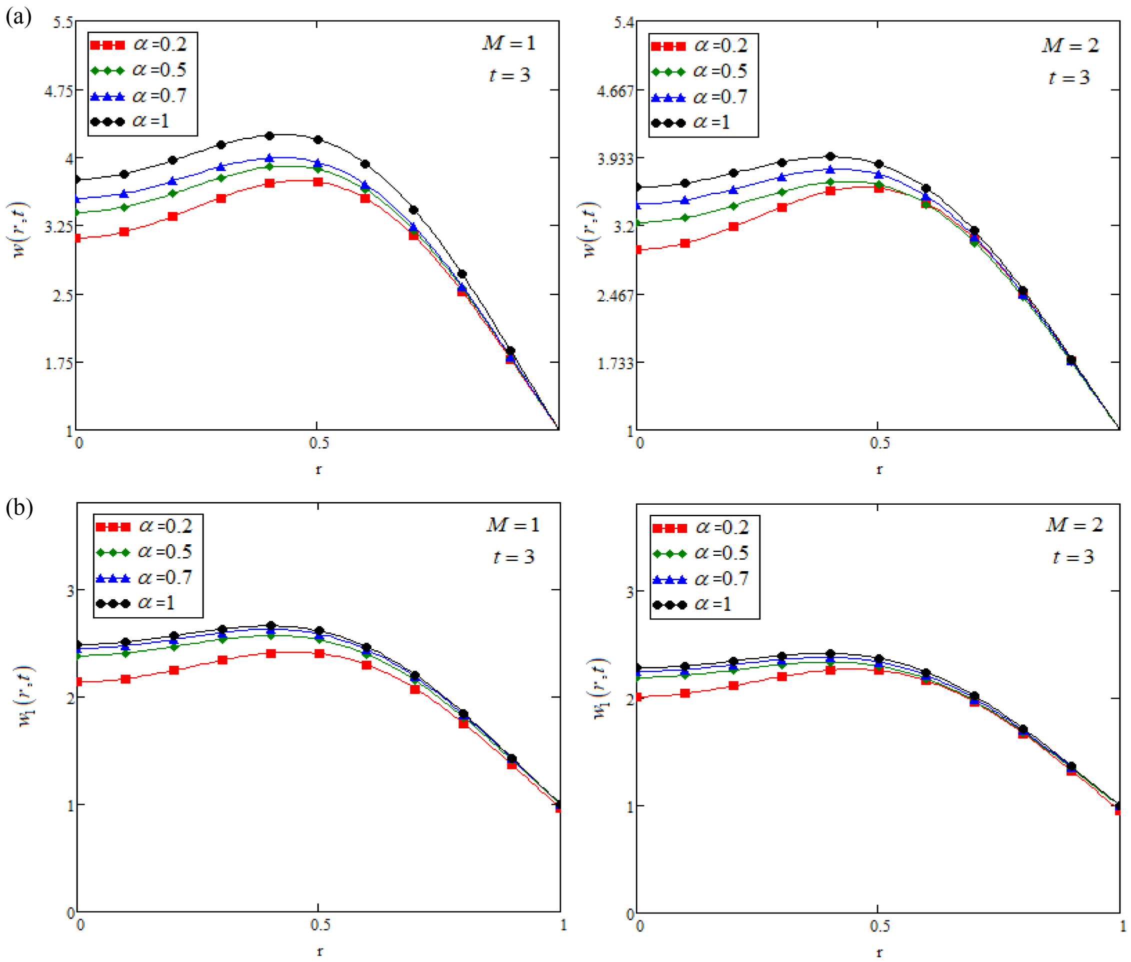

Fig. 4. (Color online) Velocity graph of Blood and Particles for different values of M for large time, when Q_0=0.3, Q_1=0.3, P_m=0.2, P_c=0.2, $\beta = 1$, $\omega = \frac{\pi}{2}$, Pr=22.64, Gr=10.

larger interval of time. From both figures, it can be concluded that with increasing magnetic parameter both the velocities (blood velocity and particle velocity) decrease. Physically, it is true because blood is an electrically conducting fluid and exhibits magnetohydrodynamic flow characteristics so with the potential of MHD the Lorentz force arising out of the flow across the magnetic lines of force acts on the constituent particles of blood and alters the hemodynamic indicators of blood flow, such type of use of magnetic field results in the prevention of blood flow, but in Fig. 3 it can be seen that for short interval of time the fractional velocity is greater than the classical velocity, while in Fig. 4 for large interval of time the classical velocity is greater than the fractional velocity. In Fig. 5, 6 the Grashoff number effect has been shown for both velocities (blood velocity and particle velocity) with respect to short and large interval of time. From both figures it can be observed that by increasing the Grashoff number both the velocities increases due to the increase in the buoyancy term because, Grashoff number represents the ratio between the buoyancy force due to spatial variation in fluid density (caused by temperature differences) to the restraining force due to the viscosity of the fluid. But for short interval of time, the fractional velocity is greater than the classical velocity as shown in Fig. 5 while in Fig. 6 the classical velocity is greater than the fractional velocity for a large interval of time. In Fig. 7, 8 the effect of Casson fluid parameter has been shown on both the velocities. By increasing the Casson fluid parameter both the velocities increases due to the fact that when the Casson fluid parameter increases so the yield stress fall through which the boundary layer thickness decreases. In Fig. 7 the fractional velocity is greater than the classical velocity for short interval of time, while in Fig. 8 the classical velocity is greater than the fractional velocity for a larger interval of time.

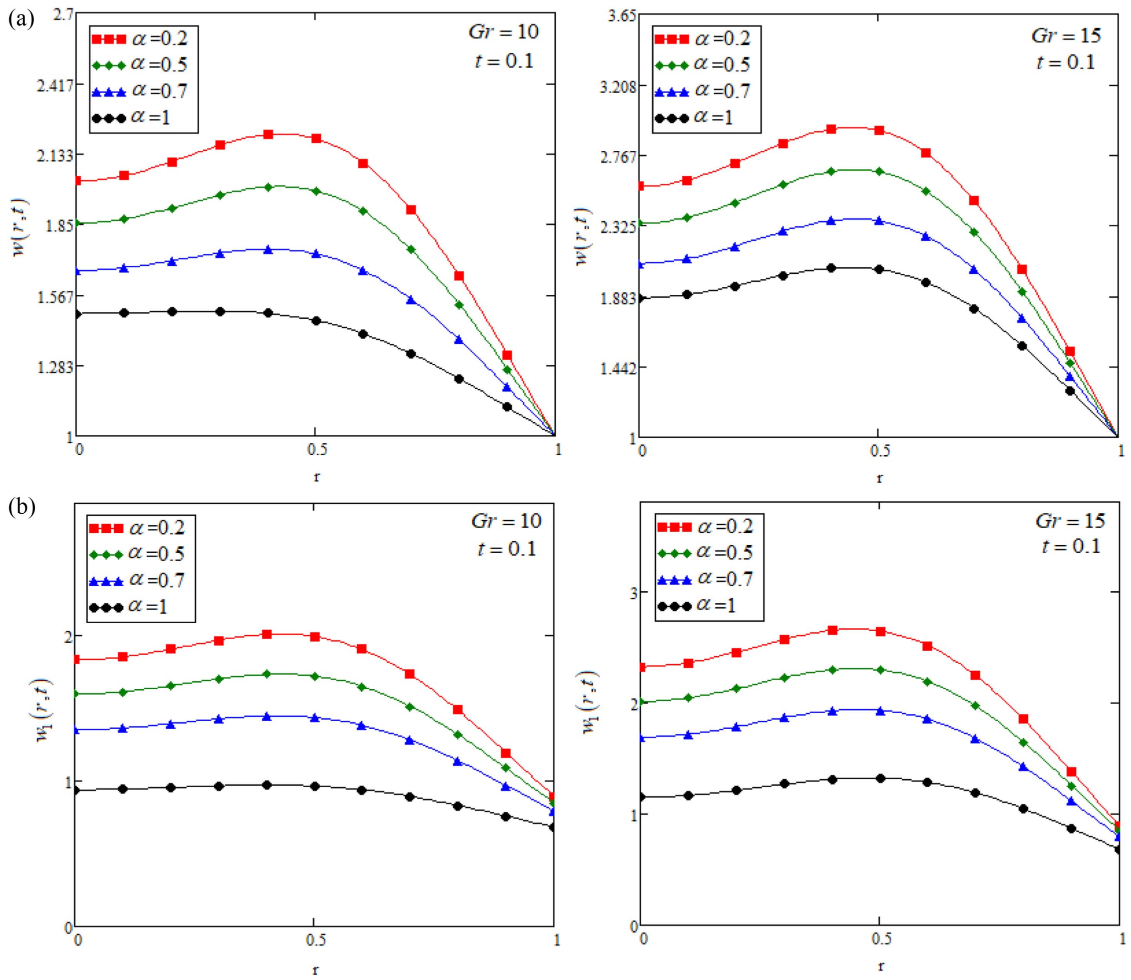

Fig. 5. (Color online) Velocity graph of Blood and Particles for different values of Gr for short time, when Q_0=0.3, Q_1=0.3, P_m=0.2, P_c=0.2, $\beta = 1$, $\omega = \frac{\pi}{2}$, Pr=22.64.

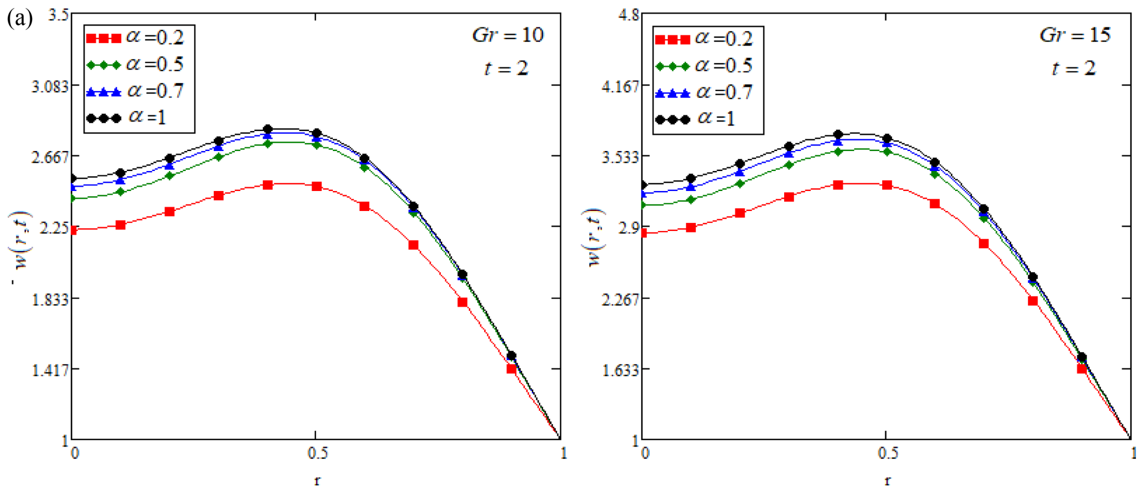

Fig. 6. (Color online) Velocity graph of Blood and Particles for different values of M for a large time, when Q_0=0.3, Q_1=0.3, P_m=0.2, P_c=0.2, $\beta = 1$, $\omega = \frac{\pi}{2}$, Pr=22.64.

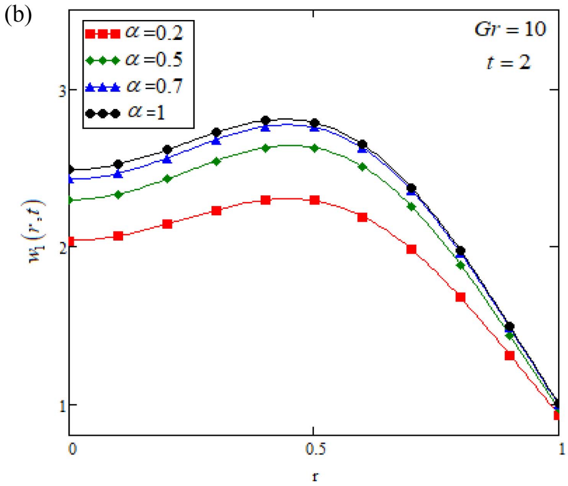

Fig. 6. (Color online) Continued.

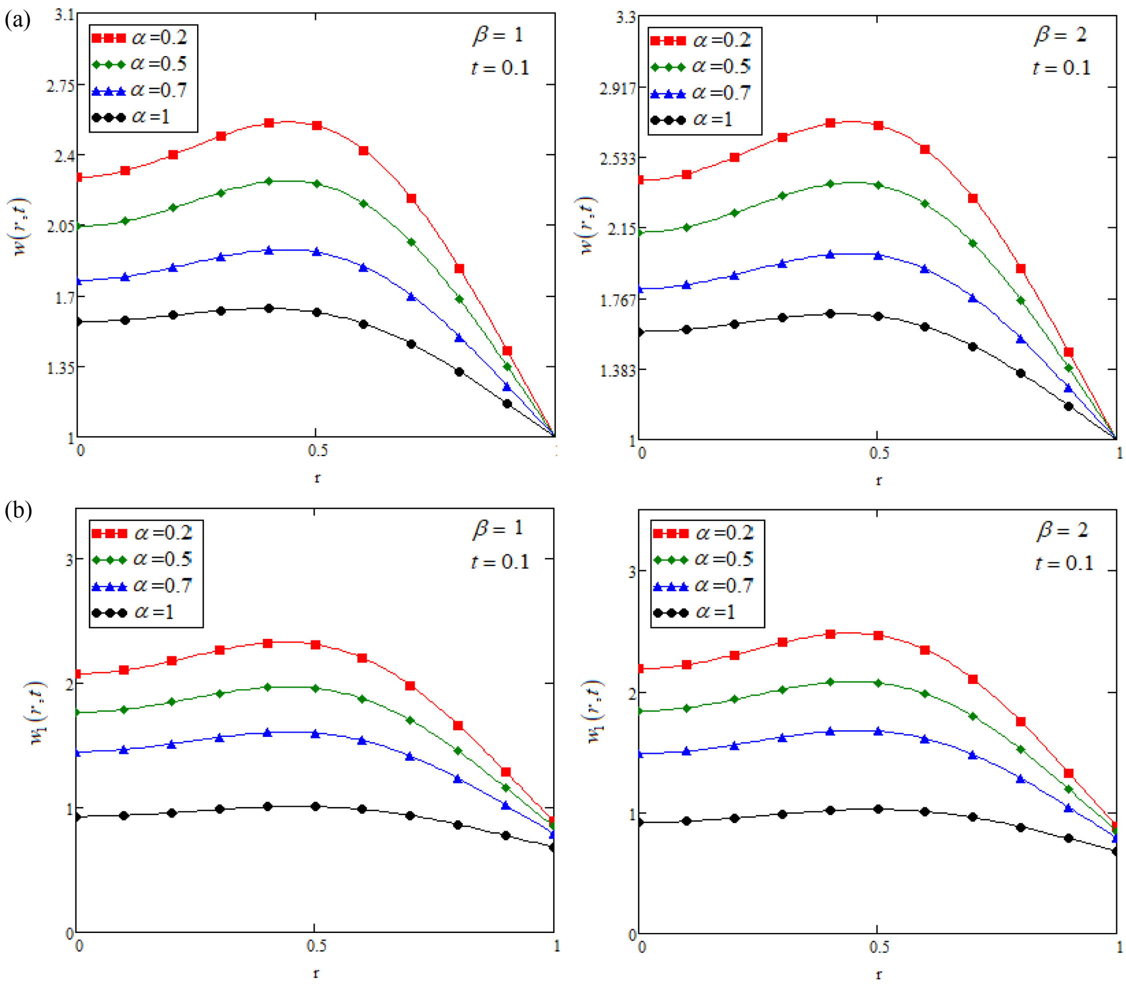

Fig. 7. (Color online) Velocity graph of Blood and Particles for different values of β for short time, when Q_0=0.3, Q_1=0.3, P_m=0.2, P_c=0.2, β= 1, $\omega = \frac{\pi}{2}$, Pr=22.64.

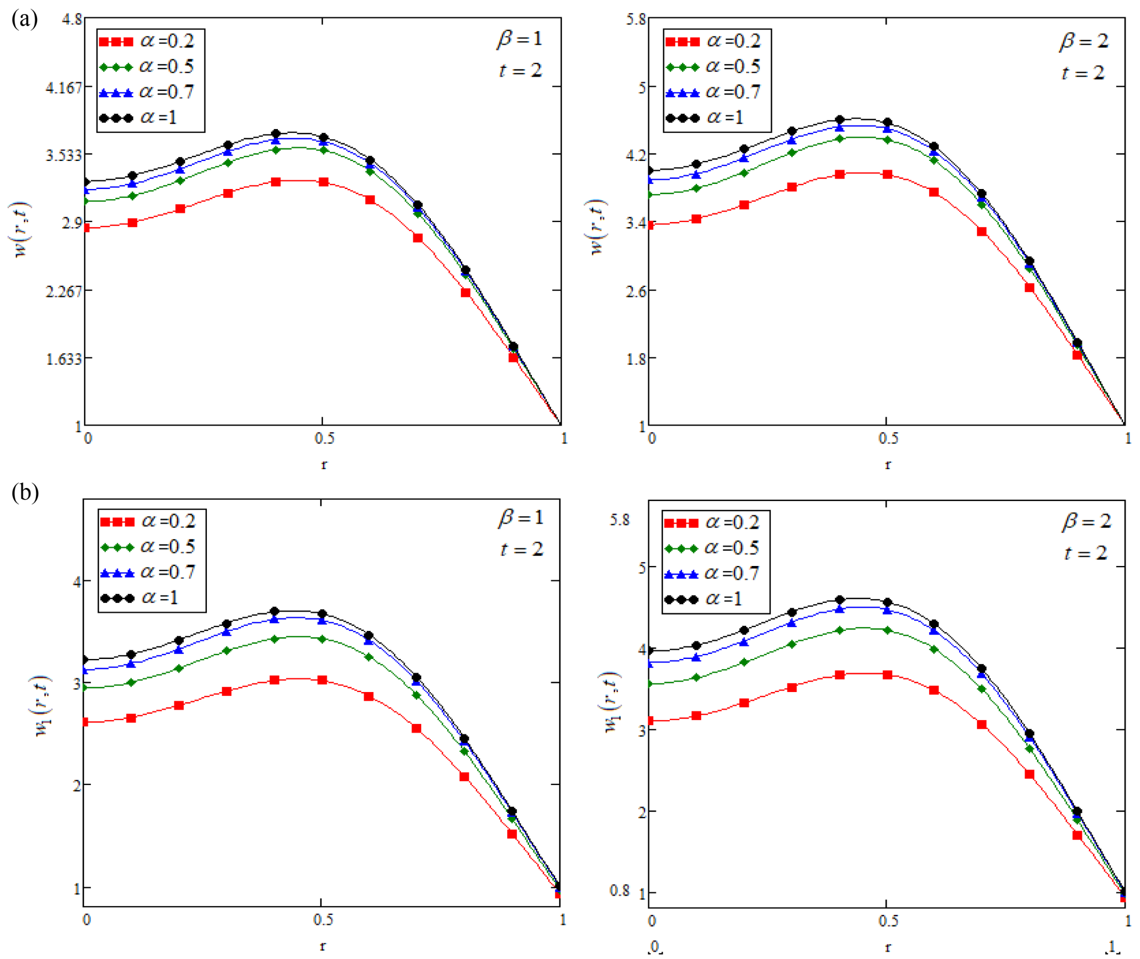

Fig. 8. (Color online) Velocity graph of Blood and Particles for different values of β for a large time, when Q_0=0.3, Q_1=0.3, P_m=0.2, P_c=0.2, β= 1, $\omega = \frac{\pi}{2}$, Pr=22.64.

5. Conclusion

- The blood flow of non-Newtonian Casson fluid with heat transfer has been discussed in narrow and small capillary vessels. These vessels were considered in the form of a cylindrical tube.
- The Caputo Fabrizio time fractional derivative has used for the solution of the problem.
- The impacts of the external magnetic field and other flow parameters on fluid velocity in the cylindrical domain have been shown.
- Closed form solutions have been obtained by using the Joint Laplace and Hankel transforms.
- The velocities increase with an increase in the Grashoff number.
- External applied magnetic field M reduces the velocity of the fluid as well as the velocity of particles and controls turbulences.
- By increasing the Casson fluid parameter β both the velocities increases.

Acknowledgement

The authors would like to acknowledge the ORIC, CUSIT for technical support in this research work.

Conflict of Interest

The authors declare that they have no conflict of interest.

Nomenclature

p : Oscillating pressure gradient
Q_0 : Amplitude of the systolic pressure gradient
Q_1 : Amplitude of the diastolic pressure gradient
w : fluid velocity in z' -direction (m/s);

r : Radial axis
μ_B : Plastic dynamic viscosity
Gr : non-dimensional Grashoff number
k_f : thermal conductivity of base fluid ($Wm^{-1}K^{-1}$);
R_0 : Radius of the cylinder
U_0 : Characteristic velocity
τ_r : Yield stress of fluid
μ : dynamic viscosity of fluid (kg m^{-1} s^{-1});
π_c : Critical value of the product based non-Newtonian model;
T fluid temperature (K);
β_T : thermal expansion coefficient of base fluid (K^{-1});
T_∞ : Ambient temperature
T_w : Wall temperature
μ_0 : magnetic permeability
υ : dynamic viscosity coefficient of base fluid;
β : Casson fluid parameter;
ρ : Density of the fluid
M : non-dimensional magnetic parameter;
ω : Angular frequency
Pr : non-dimensional Prandtl number;
B_0 : applied magnetic field;
g : acceleration due to gravity (m s^{-2});
$\vec{J}$: current density
β : Casson fluid parameter;
$\vec{E}$: electric field
$\vec{B}$: magnetic flux density
$\vec{V}$: velocity vector
σ : electrical conductivity
w_1 : magnetic particle velocity
K : Stokes constant
N : number of magnetic particles per unit volume
P_c : non-dimensional parameter for the particle concentration

References

[1] R. Botnar, G. Rappitsch, M. B. Scheidegger, D. Liepsch, K. Perktold, and P. Boesiger, J. Biomech. **33**, 137 (2000).
[2] C. W. Kerber and D. Liepsch, Am. J. Neuroradiol. **15**, 1065 (1994).
[3] P. D. Stein, A physical and physiological basis for the interpretation of cardiac auscultation: evaluations based primarily on the second sound and ejection murmurs. Blackwell/Futura (1981).
[4] E. K. Ruuge and A. N. Rusetski, J. Magn. Magn. Mater. **122**, 335 (1993).
[5] J. Plavins and M. Lauva, J. Magn. Magn. Mater. **122**, 349 (1993).
[6] J. Liu, G. A. Flores, and R. Sheng, J. Magn. Magn. Mater. **225**, 209 (2001).
[7] P. A. Voltairas, D. I. Fotiadis, and L. K. Michalis, J. Biomech. **35**, 813 (2002).
[8] M. K. Banerjee, A. Datta, and R. Ganguly, J. Nanotechnol. Eng. Med. **1**, 041005 (2010).
[9] S. Kenjereš, International Journal of Heat and Fluid Flow **29**, 752 (2008).
[10] E. E. Tzirtzilakis, Int. J. Numer. Method. Biomed. Eng. **24**, 683 (2008).
[11] J. W. Haverkort, S. Kenjereš, and C. R. Kleijn, Ann. Biomed. Eng. **37**, 2436 (2009).
[12] M. Tezer-Sezgin, C. Bozkaya, and Ö. Türk, Eng. Anal. Bound. Elem. **37**, 1127 (2013).
[13] Ö. Türk, C. Bozkaya, and M. Tezer-Sezgin, Computers & Fluids **97**, 40 (2014).
[14] K. Tzirakis, Y. Papaharilaou, D. Giordano, and J. Ekaterinaris, Int. J. Numer. Method. Biomed. Eng. **30**, 297 (2014).
[15] S. Bose and M. Banerjee, J. Magn. Magn. Mater. **385**, 32 (2015).
[16] Y. O. U. S. E. F. Haik, V. Pai, and C. J. Chen, Fluid Dynamics at Interfaces 439 (1999).
[17] F. Jaspard and M. Nadi, Physiological Measurement **23**, 547 (2002).
[18] E. E. Tzirtzilakis, Physics of Fluids **17**, 077103 (2005).
[19] T. Higashi, A. Yamagishi, T. Takeuchi, N. Kawaguchi, S. Sagawa, S. Onishi, and M. Date, Blood **82**, 1328 (1993).
[20] S. Sharma, U. Singh, and V. K. Katiyar, J. Magn. Magn. Mater. **377**, 395 (2015).
[21] L. Pauling and C. D. Coryell, Proceedings of the National Academy of Sciences **22**, 210 (1936).
[22] G. C. Hazarika and A. Sarmah, Int. J. Comput. Appl. **101**, (2014).
[23] D. S. Sankar and U. Lee, Journal of Mechanical Science and Technology **25**, 2573 (2011).
[24] B. M. Johnston, P. R. Johnston, S. Corney, and D. Kilpatrick, J. Biomech. **37**, 709 (2004).
[25] V. P. Rathod and S. Tanveer, Bull. Malays. Math. Sci. Soc. **32**, 245 (2009).
[26] F. Ali, N. A. Sheikh, I. Khan, and M. Saqib, J. Magn. Magn. Mater. **423**, 327 (2017).
[27] M. Nakamura and T. Sawada, J. Biomech. Eng. **110**, 137 (1988).
[28] T. Murata, Biorheology **20**, 471 (1982).
[29] D. W. Liepsch, Biorheology **23**, 395 (1985).
[30] L. M. Srivastava and V. P. Srivastava, J. Biomech. **17**, 821 (1984).
[31] R. K. Dash, K. N. Mehta, and G. Jayaraman, Int. J. Eng. Sci. **34**, 1145 (1996).
[32] D. S. Sankar, Int. J. Nonlinear Sci. Numer. Simul 10 (2009).
[33] S. Charm and G. Kurland, Viscometry of human blood for shear rates of 0-100,000 sec-1 (1965).
[34] E. W. Merrill, A. M. Benis, E. R. Gilliland, T. K. Sherwood, and E. W. Salzman, J. Appl. Physiol. **20**, 954 (1965).

[35] M. Motta, Y. Haik, A. Gandhari, and C. J. Chen, Bioelectrochem. Bioenerg. **47**, 297 (1998).
[36] M. Bartoszek and Z. Drzazga, J. Magn. Magn. Mater. **196**, 573 (1999).
[37] S. Ichioka, M. Minegishi, M. Iwasaka, M. Shibata, T. Nakatsuka, K. Harii, and S. Ueno, Bioelectromagnetics **21**, 183 (2000).
[38] Y. Haik, V. Pai, and C. J. Chen, J. Magn. Magn. Mater. **225**, 180 (2001).
[39] A. Kolin, Proc. Soc. Exp. Biol. Med. **35**, 53 (1936).
[40] M. F. Barnothy and I. Sümegi, In Biological effects of magnetic fields (pp. 103-126). Springer US (1969).
[41] K. Haldar and S. N. Ghosh, Indian Journal of Pure and Applied Mathematics **25**, 345 (1994).
[42] G. R. Cokelet and H. L. Goldsmith, Circulation Research **68**, 1 (1991).
[43] Z. Recebli and H. Kurt, International Journal of Heat and Fluid Flow **29**, 263 (2008).
[44] E. Gedik, H. Kurt, Z. Recebli, and A. Keçebaş, Int. J. Therm. Sci. **53**, 156 (2012).
[45] M. Sharan and A. S. Popel, Biorheology **38**, 415 (2001).
[46] R. Gorenflo and F. Mainardi, Fractional calculus: integral and differential equations of fractional order, 2008. arXiv preprint arXiv:0805.3823.
[47] S. G. Samko, A. A. Kilbas, and O. I. Marichev, Theory and Applications, Gordon and Breach, Yverdon (1993).
[48] A. Pisano, M. Rapaić, E. Usai, and Z. Jelicić, IFAC Proceedings Volumes **44**, 2436 (2011).
[49] K. A. Abro, I. Khan, and A. Tassaddiq, Math. Model. Nat. Phenom. **13**, 1 (2018).
[50] K. A. Abro, A. D. Chandio, I. A. Abro, and I. Khan, J. Therm. Anal. Calorim. 1 (2018).
[51] N. A. Shah, D. Vieru, and C. Fetecau, J. Magn. Magn. Mater. **409**, 10 (2016).
[52] S. Sharma, U. Singh, and V. K. Katiyar, J. Magn. Magn. Mater. **377**, 395 (2015).
[53] F. Ali, N. A. Sheikh, I. Khan, and M. Saqib, J. Magn. Magn. Mater. **423**, 327 (2017).
[54] F. Ali, A. Imtiaz, I. Khan, and N. A. Sheikh, J. Magn. Magn. Mater. **456**, 413 (2018).
[55] M. Kumari and G. Nath, Indian Journal of Pure and Applied Mathematics **30**, 695 (1999).
[56] S. Shaw, R. S. R. Gorla, P. V. S. N. Murthy, and C. O. Ng, International Journal of Fluid Mechanics Research **36**, (2009). DOI: 10.1615/InterJFluidMechRes.v36.i1.30.
[57] R. Piessens, The Transforms and Applications Handbook **2**, 9-1 (2000).
[58] C. F. Lorenzo and T. T. Hartley, Generalized Functions for the Fractional Calculus (Vol. 209424). National Aeronautics and Space Administration, Glenn Research Center (1999).